

Supporting information

1 Instrument Parameters and Formula Details:

1.1 Characterization

X-ray diffraction (XRD, Rigaku-D/max-2500, Cu K α radiation) was used to confirm the composition of the phases, which were scanned from 5° to 75°, the scanning speed is 5°/min. Observation of morphological characteristics of samples using JEOL JEM-7800 scanning electron microscope (SEM), the acceleration voltage during the test was 10 kV. The sample used for SEM testing was the directly grown BiOBr film, which was cut into small pieces of approximately 0.1 cm² and then attached to the sample stage. The binding energies of the sample elements were detected using an X-ray photoelectron spectrometer (XPS, Thermo Fisher-ESCALAB 250XI). The microstructure of the samples was characterized by transmission electron microscopy (TEM) on a Thermo Fisher Scientific Talos F200i instrument at an accelerating voltage of 200 kV. Both conventional TEM imaging and high-resolution TEM (HRTEM) imaging were employed to analyze the overall morphology and the atomic lattice structure, respectively. The samples used for TEM testing were prepared by gently scraping off the BiOBr film grown on FTO, dispersing it in ethanol, and ultrasonically treating it for 10 min, followed by dripping it onto a copper web supported by a ultrathin carbon film. The ultraviolet photoelectron spectroscopy (UPS) test of the sample obtained the secondary cut-off edge, from which the work function was calculated. Specifically, the sample preparation method for UPS is as follows: the BiOBr films grown directly on FTO glass were used without further treatment, and the UPS measurements were performed using a He I (21.22 eV) UV light source. Energy-dispersive X-ray spectroscopy (EDS) is used to confirm the content of elements in the material. The functional groups of the samples were characterized by Fourier transform infrared (FT-IR) spectroscopy using a Shimadzu IRTracer-100 spectrometer.

$$E_g = 1240/\lambda_{Absorp\ Edge} \quad (1)$$

$$\alpha hv = A(hv - E_g)^{n/2} \quad (2)$$

A is a constant, $h\nu$ represents the photon energy, α is the absorption coefficient and E_g is the band gap energy. BiOBr is an indirect bandgap semiconductor, so the value of n is 4. Steady-state photoluminescence (PL) was used to analyze the carrier recombination situation of the samples.

1.2 Photoelectrochemical Characterization

The photoelectrochemical performance of the samples was evaluated using a

constant electrochemical workstation (CHI760E, Changhua, Shanghai, China) with Ag/AgCl as the reference electrode and a platinum (Pt) sheet as the counter electrode using a 300 W xenon lamp to simulate a solar light source and a 1.5 G filter to control the light intensity at 100 mW cm⁻². The electrolyte is a 0.1 M Na₂SO₄. The measured potential is converted to the reversible hydrogen electrode (RHE) value through the following formula^[37]:

$$E_{\text{RHE}} = E_{\text{Ag/AgCl}} + 0.059 * \text{pH} + 0.197 \text{ V} \quad (3)$$

The current density-voltage (J-V) curves of the samples were measured using linear scanning voltammetry (LSV). An AC bias voltage of 0.65 V was applied to the sample to obtain the electrochemical impedance spectrum (EIS) of the sample. To analyze the changes in the energy band structure of the samples, the Mott-Schottky (M-S) curves of the samples were measured, which were calculated as follows^[38]:

$$1/c^2 = 2/\varepsilon\varepsilon_0eA^2N_d(V-V_{\text{fb}}-K_B T/e) \quad (4)$$

C is the space charge capacitance, ε the vacuum dielectric constant, ε_0 is the relative permittivity of BiOBr, e is the fundamental charge, A is the effective working area of the working electrode (1 cm²), V is the applied bias voltage, V_{fb} is the flat band potential. K_B is the Boltzmann constant (1.38×10^{-23} J/K), T is the temperature (K).

To understand the conversion efficiency of the sample photogenerated electrons, applied bias photon to current efficiency (ABPE) was tested with the following equation^[39]:

$$\text{ABPE} (\%) = J_p(1.23-V_{\text{bias}})/P_{\text{light}} \times 100 \% \quad (5)$$

Where J_p , V_{bias} and P_{light} represent the photocurrent density, the applied bias voltage and the incident light density respectively.

The CV data were measured by cyclic voltammetry (CV) with a scan rate of 50-80 mV/s. Based on the obtained data, the double-layer capacitance C_{dl} was further calculated. Since the electrolyte is slightly neutral, C_s represents the specific capacitance per unit area, with a value of 60 mF/cm². The electrochemical active surface area (ECSA) was calculated accordingly.

$$\text{ECSA} = C_{\text{dl}}/C_s \quad (6)$$

2 List of Figures and Tables:

Fig. S1 2% Ga³⁺ doped BiOBr sample: (a, b) SEM images; (c) total spectrum; (d) - (g) element distribution

Fig. S2 (a) XRD patterns of the conventional Ga³⁺ doped and sorbitol-mediated BiOBr samples; (b) a detailed enlarged view of (a)

Fig. S3 Fourier transforms infrared (FT-IR) spectra of mannitol- and sorbitol-mediated samples and their synergistic Ga³⁺-doped counterparts

Fig. S4 XPS spectrum of sorbitol-mediated synergistic 2% Ga³⁺-doped samples. (a) O 1s; (b) C 1s

Fig. S5 EDS spectrum of sorbitol-mediated synergistic 2% Ga³⁺-doped samples. (a) Scan area; (b)–(e) elemental distribution; (f) total spectrum

Fig. S6 (a) and (b) show the UV tauc plots for mannitol- and sorbitol-mediated samples, and their synergistic Ga³⁺-doped counterparts, respectively

Fig. S7 Characterization of conventionally 2% Ga³⁺-doped BiOBr (without chiral inducer): (a) UV-vis absorption and Tauc plot; (b) C_{dl} fitting. (c, d) PL comparison between the conventionally doped sample and chirality-mediated undoped BiOBr: (c) mannitol-mediated; (d) sorbitol-mediated

Fig. S8 (a) LSV, (b) ABPE, (c) I-T, and (d) EIS of the conventionally 2% Ga³⁺-doped BiOBr (without chiral inducer)

Fig. S9 (a) and (b) represent the ABPE diagrams for mannitol- and sorbitol-mediated samples, and their synergistic Ga³⁺-doped counterparts, respectively

Fig. S10 CV diagrams of mannitol-mediated and synergistic Ga³⁺-doped samples

Fig. S11 CV diagrams of sorbitol-mediated and synergistic Ga³⁺-doped samples

Fig. S12 (a) and (b) show the intrinsic LSV curves for mannitol- and sorbitol-mediated samples and their Ga³⁺-doped counterparts, respectively

Fig. S13 Intrinsic LSV curve of the conventionally 2% Ga³⁺-doped BiOBr sample (prepared without any chiral inducer)

Fig. S14 Equivalent circuit diagram corresponding to Fig. 8(c), (d)

Fig. S15 (a) Secondary cutoff edge measured by UPS for sorbitol-mediated BiOBr; (b) secondary cutoff edge measured by UPS for sorbitol-mediated BiOBr synergised with a 2% Ga³⁺-doped concentration sample

Fig. S16 Schematic diagram of the bandgap width plotted based on the approximate equivalent conduction band position derived from the Mott-Schottky flat-rate potential and the ultraviolet tauc plot

Tab. S1: Elemental content map of BiOBr mediated by sorbitol with 2% Ga³⁺ doping concentration as determined by EDS analysis

Tab. S2: Elemental content map of conventionally 2% Ga³⁺-doped BiOBr (without chiral inducer) as determined by EDS analysis

Tab. S3: ECSA profiles of BiOBr and its synergistic Ga³⁺-doped samples at varying concentrations, mediated by sorbitol and mannitol

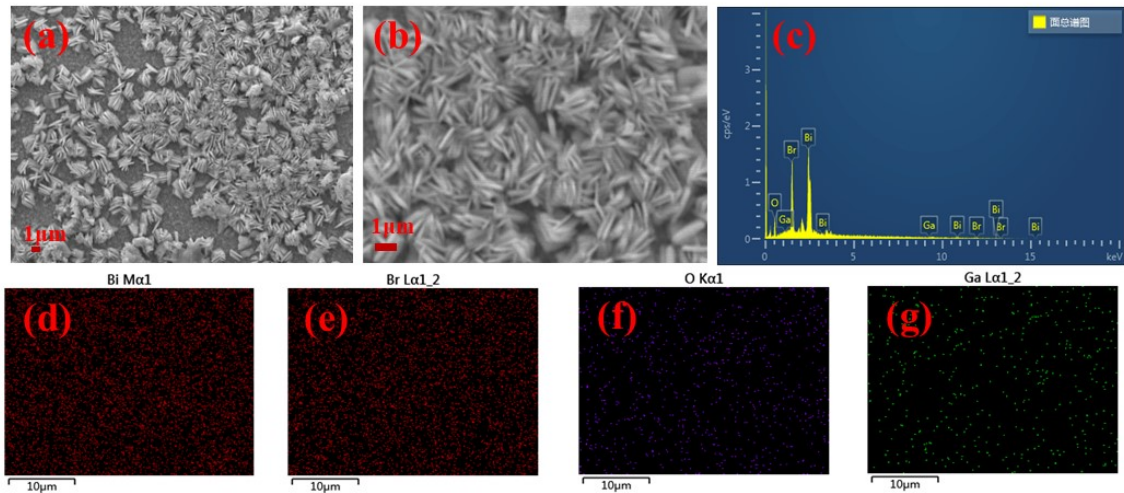


Fig. S1 2% Ga³⁺ doped BiOBr sample: (a, b) SEM images; (c) total spectrum; (d) - (g) element distribution

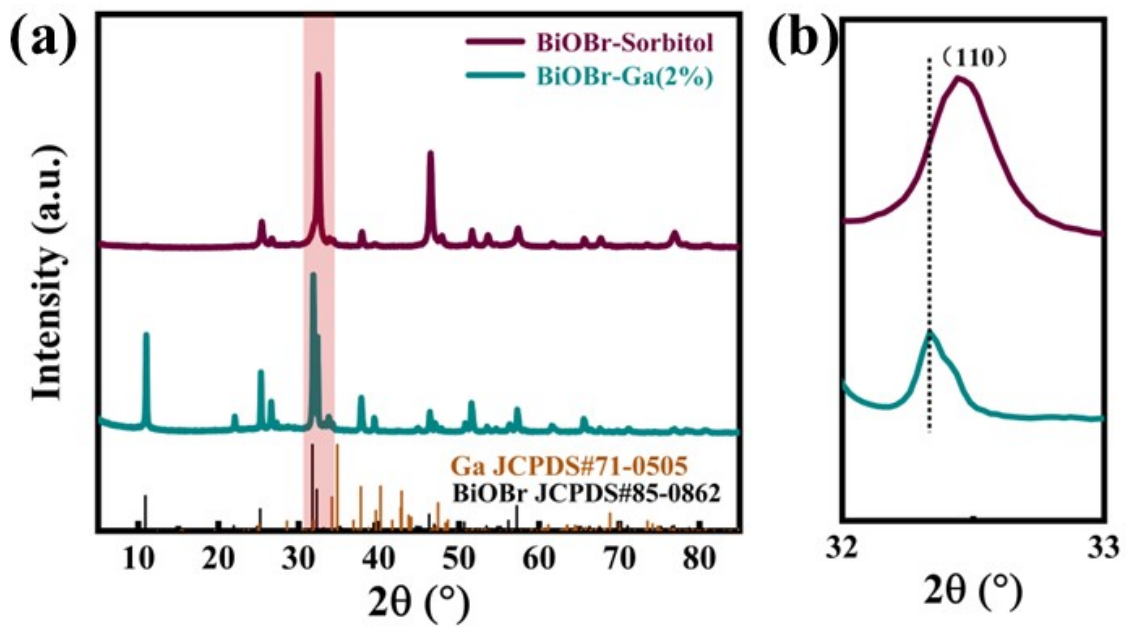


Fig. S2 (a) XRD patterns of the conventional Ga³⁺ doped and sorbitol-mediated BiOBr samples; (b) a detailed enlarged view of (a)

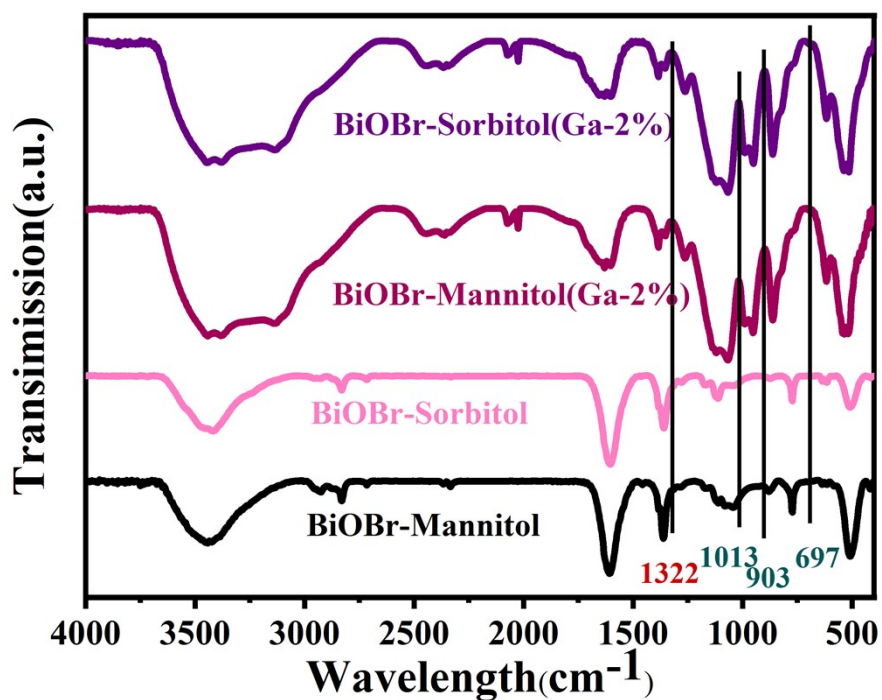


Fig. S3 Fourier transforms infrared (FT-IR) spectra of mannitol- and sorbitol-mediated samples and their synergistic Ga^{3+} -doped counterparts

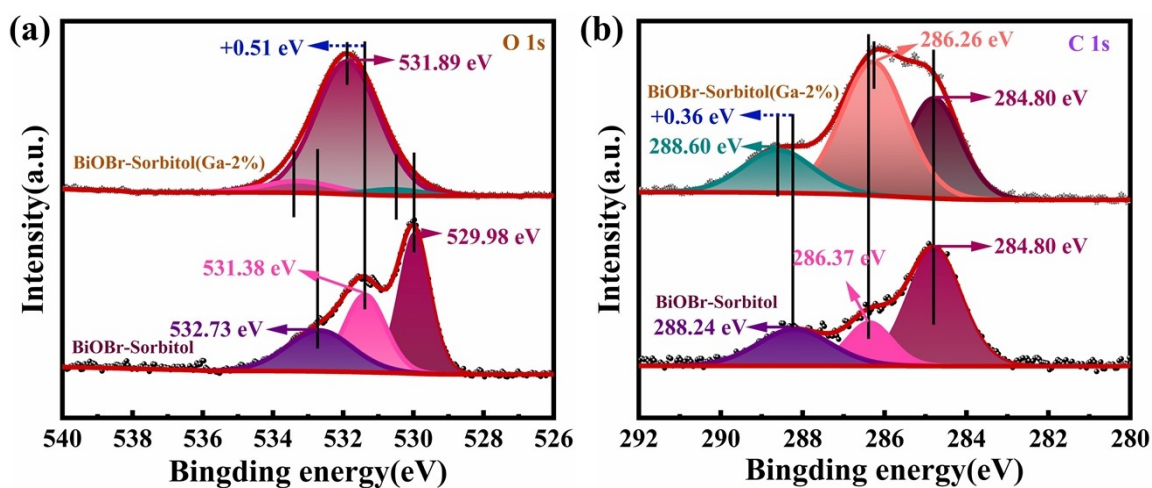


Fig. S4 XPS spectrum of sorbitol-mediated synergistic 2% Ga^{3+} -doped samples. (a) O 1s; (b) C 1s

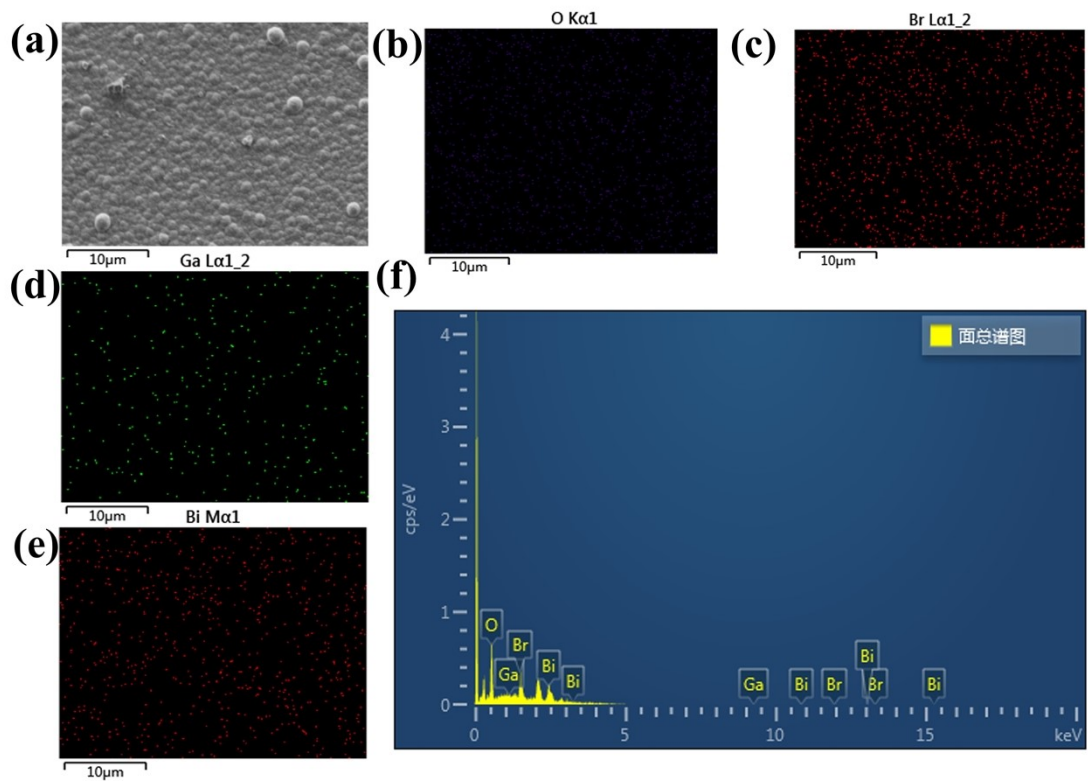


Fig. S5 EDS spectrum of sorbitol-mediated synergistic 2% Ga³⁺-doped samples. (a) Scan area; (b)–(e) elemental distribution; (f) total spectrum

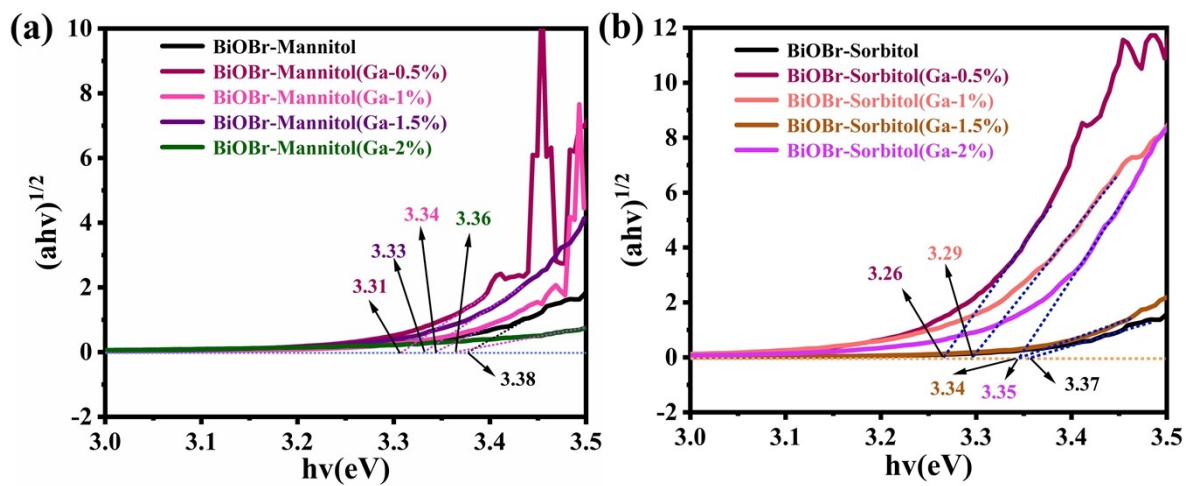


Fig. S6 (a) and (b) show the UV tauc plots for mannitol- and sorbitol-mediated samples, and their synergistic Ga³⁺-doped counterparts, respectively

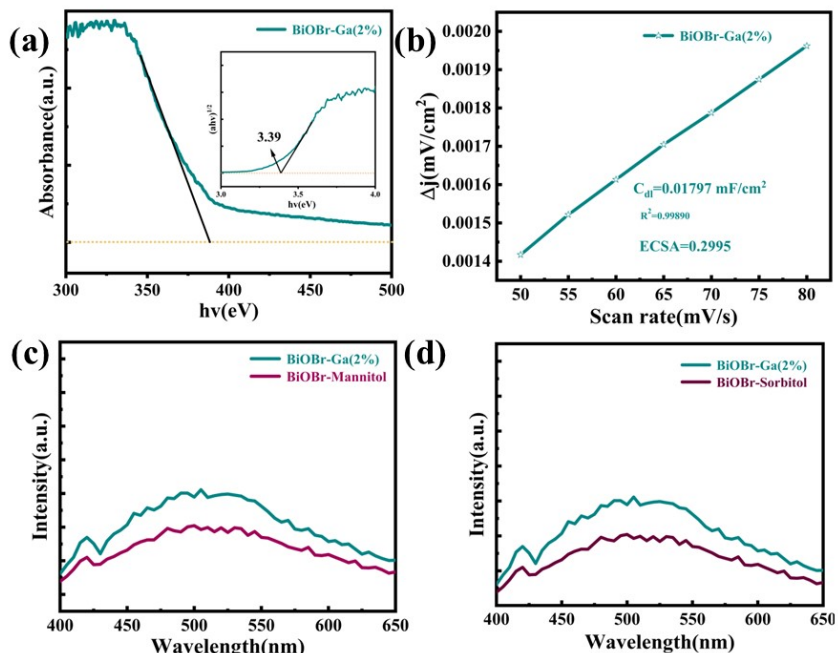


Fig. S7 Characterization of conventionally 2% Ga^{3+} -doped BiOBr (without chiral inducer): (a) UV-vis absorption and Tauc plot; (b) C_{dl} fitting. (c, d) PL comparison between the conventionally doped sample and chirality-mediated undoped BiOBr: (c) mannitol-mediated; (d) sorbitol-mediated

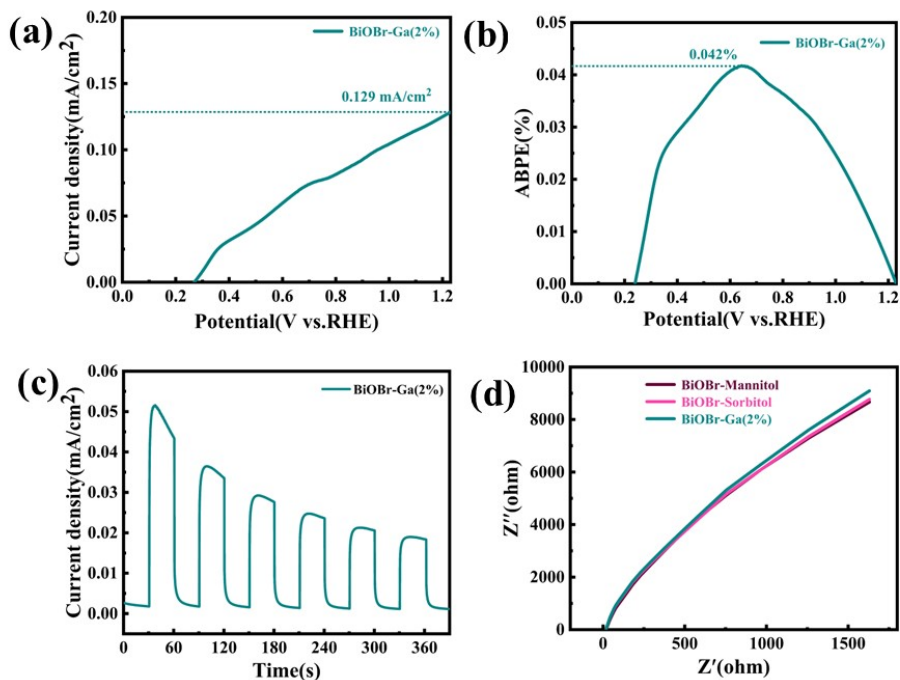


Fig. S8 (a) LSV, (b) ABPE, (c) I-T, and (d) EIS of the conventionally 2% Ga^{3+} -doped BiOBr (without chiral inducer)

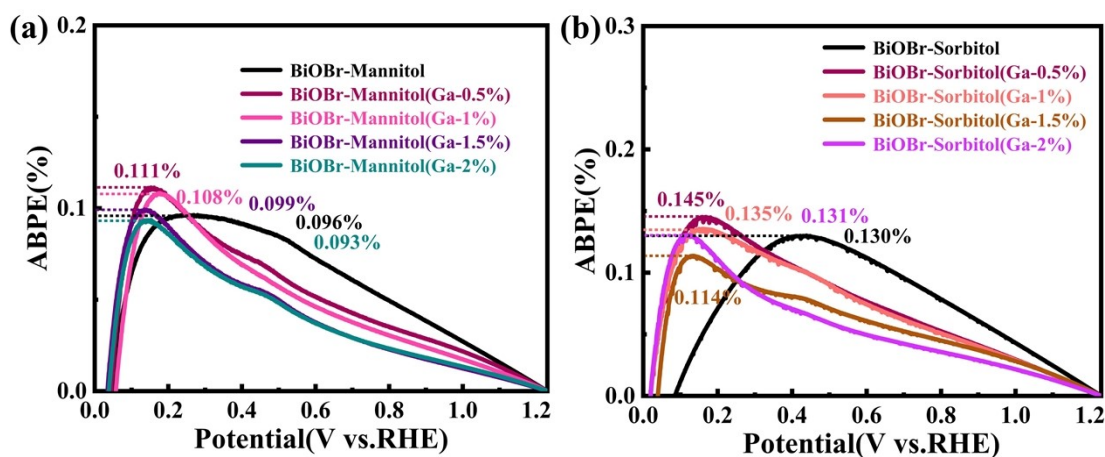


Fig. S9 (a) and (b) represent the ABPE diagrams for mannitol- and sorbitol-mediated samples, and their synergistic Ga³⁺-doped counterparts, respectively

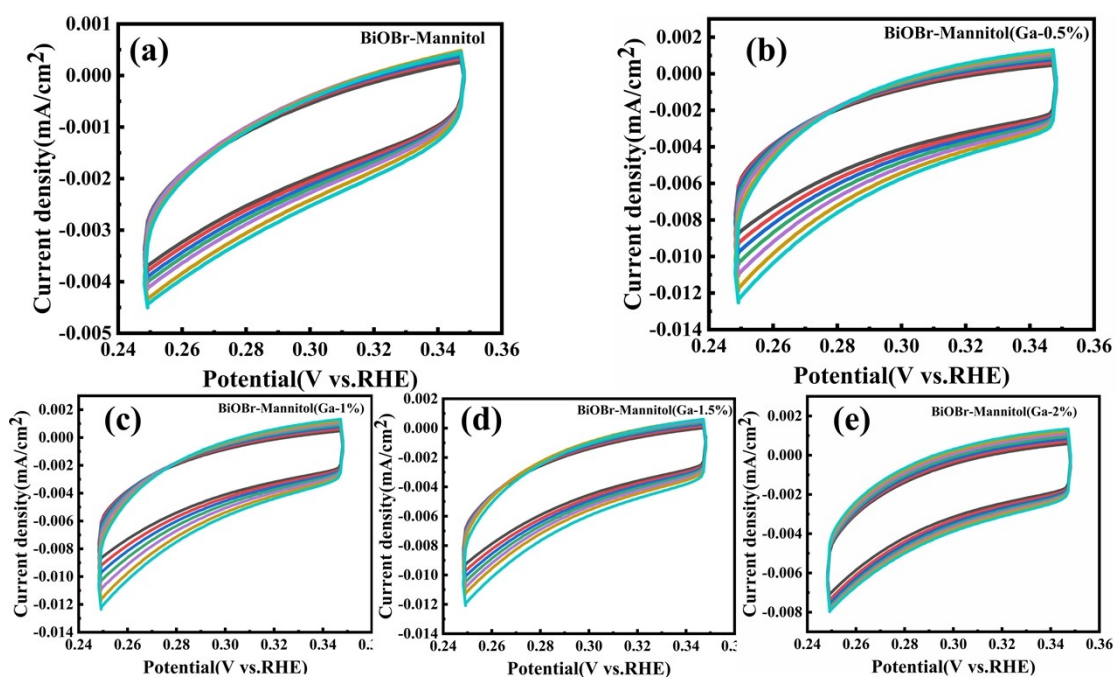


Fig. S10 CV diagrams of mannitol-mediated and synergistic Ga³⁺-doped samples

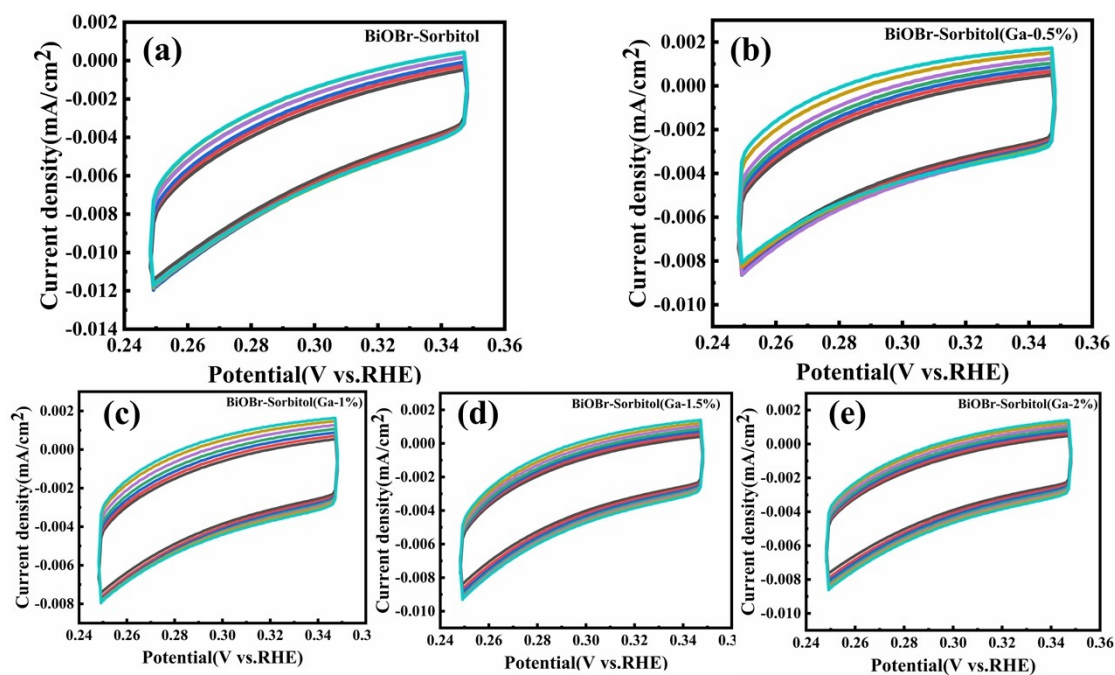


Fig. S11 CV diagrams of sorbitol-mediated and synergistic Ga^{3+} -doped samples

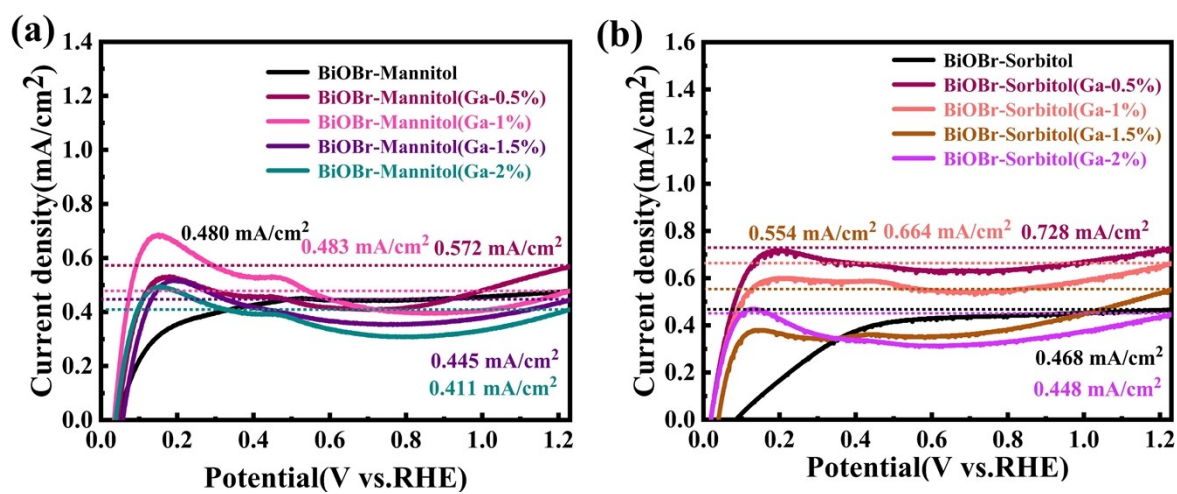


Fig. S12 (a) and (b) show the intrinsic LSV curves for mannitol- and sorbitol-mediated samples and their Ga^{3+} -doped counterparts, respectively

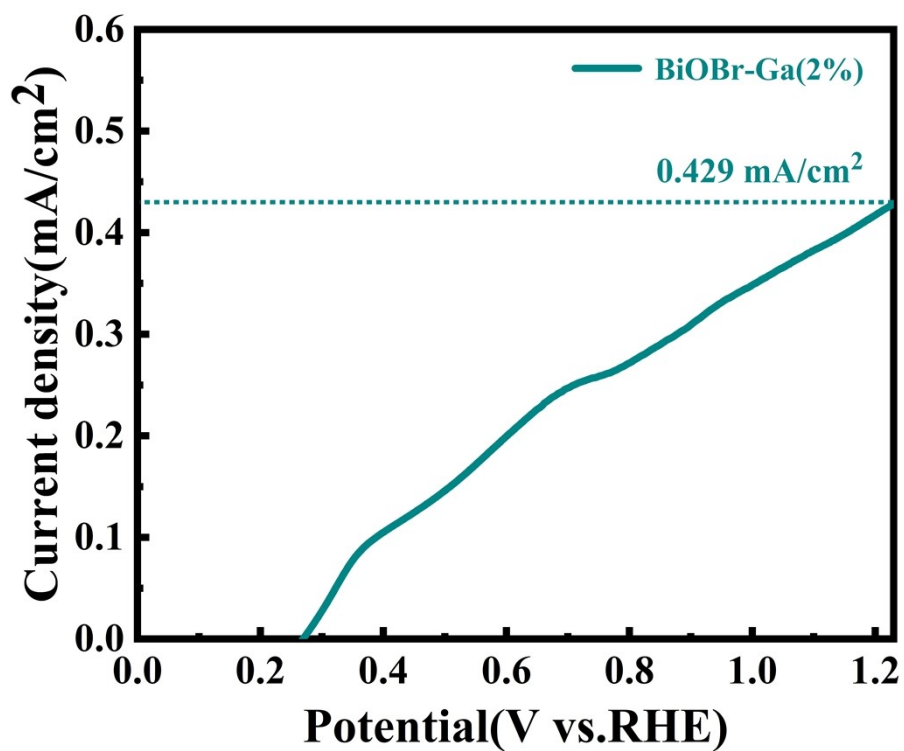


Fig. S13 Intrinsic LSV curve of the conventionally 2% Ga³⁺-doped BiOBr sample (prepared without any chiral inducer)

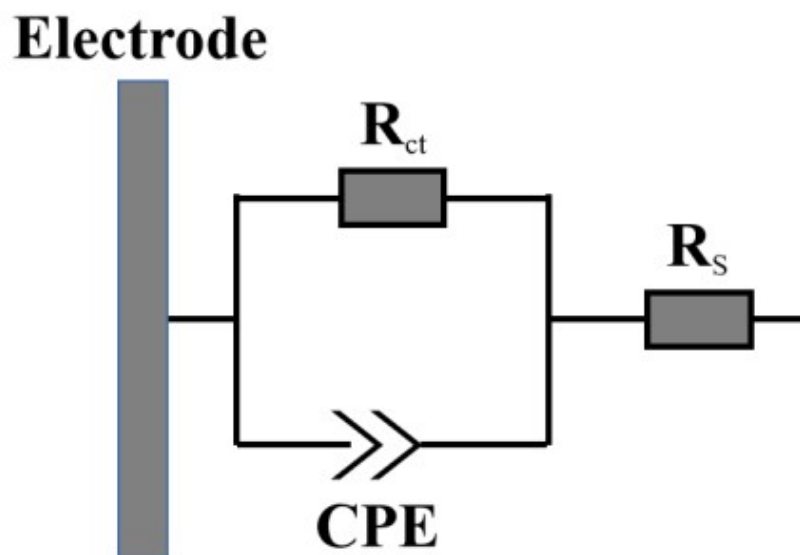


Fig. S14 Equivalent circuit diagram corresponding to Fig. 8(c), (d)

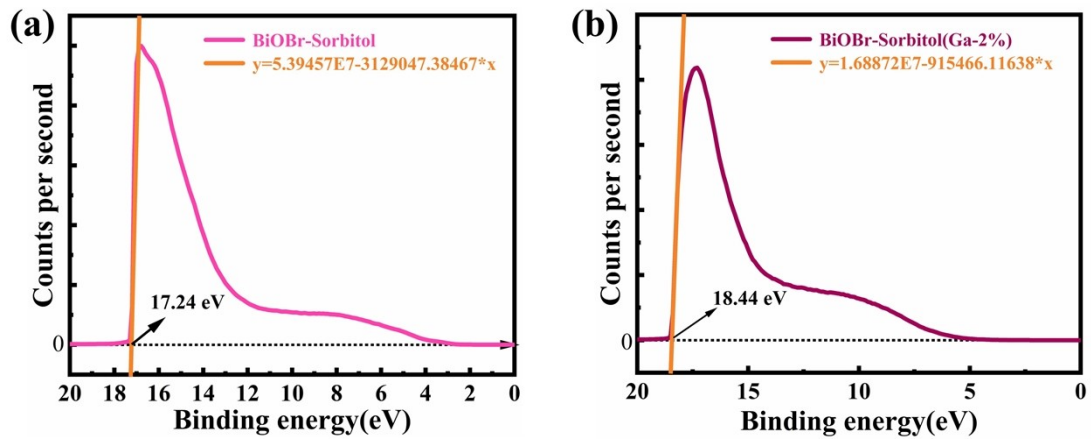


Fig. S15 (a) Secondary cutoff edge measured by UPS for sorbitol-mediated BiOBr; (b) secondary cutoff edge measured by UPS for sorbitol-mediated BiOBr synergised with a 2% Ga³⁺-doped concentration sample

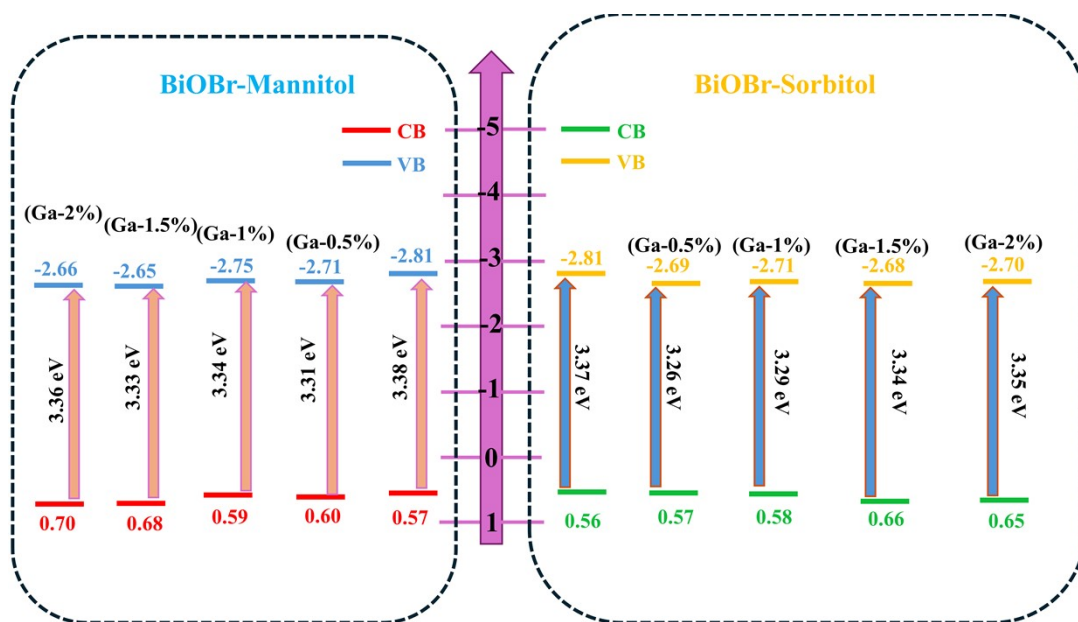


Fig. S16 Schematic diagram of the bandgap width plotted based on the approximate equivalent conduction band position derived from the Mott-Schottky flat-rate potential and the ultraviolet tauc plot

Tab. S1: Elemental content map of BiOBr mediated by sorbitol with 2% Ga³⁺ doping concentration as determined by EDS analysis

元素	wt%	wt% Sigma
O	15.69	1.44
Ga	0.17	0.91
Br	21.18	2.20
Bi	62.96	3.18
总量:	100.00	

Tab. S2: Elemental content map of conventionally 2% Ga³⁺-doped BiOBr (without chiral inducer) as determined by EDS analysis

元素	wt%	wt% Sigma
O	8.53	0.61
Ga	0.57	0.38
Br	23.67	0.74
Bi	67.23	0.94
总量:	100.00	

元素	wt%	wt% Sigma
O	10.65	0.70
Ga	0.05	0.45
Br	23.19	0.81
Bi	66.11	1.06
总量:	100.00	

Tab. S3: ECSA profiles of BiOBr and its synergistic Ga³⁺-doped samples at varying concentrations, mediated by sorbitol and mannitol

Name	BiOBr-Mannitol	BiOBr-Mannitol(Ga-0.5%)	BiOBr-Mannitol(Ga-1%)	BiOBr-Mannitol(Ga-1.5%)	BiOBr-Mannitol(Ga-2%)
C_{dl} (mF/cm²)	0.01998	0.03541	0.03519	0.02997	0.02486
ECSA (pH = 6.8, C_s = 60 μF/cm²)	0.3330	0.5902	0.5865	0.4995	0.4143
Name	BiOBr-Sorbitol	BiOBr-Sorbitol(Ga-0.5%)	BiOBr-Sorbitol(Ga-1%)	BiOBr-Sorbitol(Ga-1.5%)	BiOBr-Sorbitol(Ga-2%)
C_{dl} (mF/cm²)	0.02486	0.03079	0.03068	0.02957	0.02911
ECSA (pH = 6.8, C_s = 60 μF/cm²)	0.4143	0.5132	0.5113	0.4928	0.4852